Polymer Journal (2017) 49, 497–502

www.nature.com/pj

ORIGINAL ARTICLE

Influence of the viscosity ratio of polyacrylonitrile/poly (methyl methacrylate) solutions on core–shell fibers prepared by coaxial electrospinning

Navaporn Kaerkitcha[1], Surawut Chuangchote[2,3], Kan Hachiya[1] and Takashi Sagawa[1]

The range of viscosity ratios suitable for the fabrication of core–shell fibers was studied using a mixture of poly(methyl methacrylate) and polyacrylonitrile as a test system. The effect of the viscosity ratio of the outer/inner solutions on the morphology of the obtained core–shell fibers was studied by altering the concentrations of the two polymer solutions. The different viscosity ratios of the outer/inner solutions affected the uniform core–shell structure formation, overall diameter and wall thickness of the obtained fibers, which was confirmed by scanning electron microscopic and transmission electron microscopic observations. It was found that a viscosity ratio of the outer/inner solutions ranging from 1.22 to 2.82 resulted in uniform core–shell morphologies of the resultant electrospun fibers.
Polymer Journal (2017) **49,** 497–502; doi:10.1038/pj.2017.8; published online 22 February 2017

INTRODUCTION

The preparation of nanofibers with core–shell structures is one of the most interesting strategies for changing the physical and functional properties of conventional single nanofibers, which have been used in many applications. Potential applications of these core–shell nanostructures in the biomedical field include nanofiber surface functionalization without affecting the core material[1] and biomolecular drug delivery.[1,2] Furthermore, applications for these materials have been explored in the field of energy-related materials, devices and/or processes, including electrodes for supercapacitors,[3] lithium-ion rechargeable batteries,[4–6] photovoltaic cells,[7] capacitive deionization,[8] size-selective screening,[9] photocatalysts[10] and conductive nanowires or nanocables.[11,12]

Among the techniques used to fabricate ultrafine nanofibers with core–shell structures are self-assembly, template synthesis, chemical vapor deposition and electrospinning.[1,13] Electrospinning has attracted considerable attention because it requires only one step and allows easy control of fiber dimensions through the adjustments of electrospinning conditions of various materials, in addition to the precise regulation of the process instruments. There are various kinds of electrospinning setups, such as direct electrospinning, emulsion electrospinning and coaxial electrospinning. Emulsion electrospinning enables the preparation of core–shell nanofibers from a single nozzle due to the immiscibility of the precursor solution, which causes phase separation between the different materials.[13–16] Compared with emulsion electrospinning, electrospinning with coaxial nozzles is more interesting because of its high reproducibility, which is caused by its specially designed multichannel spinneret.[13,17] Moreover, it has other advantages. For example, non-electrospinnable materials can also be applicable to this technique when used in combination with electrospinnable ones. Core and shell materials also can be designed for a wide range of applications. In addition, this technique allows the formation of hollow structures by a post-spinning removal of the core polymer. The hollow nanofibers produced by this technique can be improved in terms of their specific surface area without chemical modification, which allows them to maintain their chemical stability.[8]

There are several reports that have studied the process parameters (for example, solution flow rate, applied voltage, collection distance) and fluid properties (for example, polymer concentration and viscosity, solvent composition, solution conductivity) of single nanofibers prepared by direct electrospinning.[18–26] For core–shell nanofibers fabricated by coaxial electrospinning, many studies have paid attention to their applications and the methods for improving their surface area, which could increase the performance of the obtained nanofibers. Lee *et al.*[27] fabricated hollow polymeric fibers using coaxial electrospinning with an inner solution of silicone oil and an outer polymer solution. They found that the diameter and wall thickness of the obtained hollow fibers could be controlled by varying the fluid properties, including the dielectric constant of the solvents, concentration of the polymer solution, molecular weights of the polymers and viscosity of the inner silicone oil phase. Pham *et al.*[28] studied the effect of core and shell flow rates on the morphology of

[1]Department of Fundamental Energy Science, Graduate School of Energy Science, Kyoto University, Kyoto, Japan; [2]The Joint Graduate School of Energy and Environment, King Mongkut's University of Technology Thonburi, Bangkok, Thailand and [3]Nanoscience and Nanotechnology Graduate Program, Faculty of Science, King Mongkut's University of Technology Thonburi, Bangkok, Thailand
Correspondence: Professor T Sagawa, Department of Fundamental Energy Science, Graduate School of Energy Science, Kyoto University, Yoshida-honmachi, Sakyo-ku, Kyoto 606-8501, Japan.
E-mail: sagawa@energy.kyoto-u.ac.jp
Received 6 September 2016; revised 30 December 2016; accepted 12 January 2017; published online 22 February 2017

alginate hollow microfibers. They found that, at a constant shell flow rate, the internal diameter increased and wall thickness decreased by increasing the core flow rate. Sun *et al.*[29] studied the processing of core–shell nanofibers/mesofibers by the co-electrospinning of two materials, and they demonstrated that suitable selections of concentration, polymer molecular weights and solution conductivities allowed them to control the diameter of the coaxial fibers. However, there has been no research clarifying the relationship between the viscosity of the outer and inner fluids. In this study, we sought to find the suitable combination of fluid viscosities, in terms of viscosity ratio of outer/inner polymer solutions, through the use of the polyacrylonitrile (PAN, outer fluid) and poly(methyl methacrylate) (PMMA, inner fluid) solutions as a model system. These two polymers are well known for their electrospinnability. Moreover, these two polymers have been used to fabricate core–shell fibers for various applications (for example, hollow carbon nanofibers). The phenomenon of core–shell structure formation using different viscosity ratios was discussed. The knowledge from this work can be applied to other combinations of polymers with different molecular weights and concentrations. By determining the outer and inner polymer viscosities and designing the system within the optimum range of outer/inner viscosity ratio, fibers with good core–shell morphology can be obtained without the requirement of further experimental steps.

EXPERIMENTAL PROCEDURE

Preparation of the electrospun fibers

Core–shell composite fibers were fabricated by the coaxial electrospinning of PMMA (Mw: 996 000 g mol^{-1}, Sigma-Aldrich, St Louis, MO, USA) in the inner core solution and PAN (Mw: 150 000 g mol^{-1}, Sigma-Aldrich) in the outer shell solution. The polymers were dissolved separately in *N,N*-dimethylformamide (99.5%, Wako Pure Chemical Industries, Ltd., Osaka, Japan), and the resulting solutions were subject to magnetic stirring at room temperature overnight. To investigate the optimum range of viscosity ratio for the preparation of core–shell fibers, we had to investigate the optimum range of viscosity of both the core and shell solutions that could be used for the fabrication of fibers of both polymers with good morphology. The single fibers prepared from the two polymer solutions were fabricated by single-nozzle electrospinning (gauge 20, diameter 0.9 mm, Terumo Co., Tokyo, Japan). The concentrations of PMMA and PAN investigated in this work ranged from 3 to 12 wt% and from 6 to 12 wt%, respectively. The electrospinning was carried out under an applied electrical voltage of 15 kV onto a stable aluminum foil collector (nozzle-to-collector distance = 15 cm) with a solution-pumped flow rate of 1.0 ml h^{-1}. The core–shell composite fibers were prepared by in-house–designed coaxial electrospinning, in which inner and outer diameter of the nozzles were 0.58 and 1.20 mm, respectively. The core and shell solutions were pumped at the same flow rate of 1.0 ml h^{-1}. The other electrospinning conditions were kept the same, with the single-nozzle electrospinning being performed at ambient temperature (25 °C) with a relative humidity of 30%.

Characterizations

Viscosities of the polymer solutions were measured in terms of dynamic viscosity because the flow of the polymer solutions out of the electrospinning nozzle was continuous throughout the electrospinning process. The dynamic viscosities of the PAN and PMMA solutions were measured by an Ostwald viscometer (No. 3, C = 0.0953, Kusano Scientific Instrument MFG, Co., Ltd., Tokyo, Japan). The Ostwald viscometer works on the basis of the Hagen–Poiseuille law: the volume V of a homogeneous fluid having a viscosity η passing for a time t through a capillary tube having a length L and a radius r at a pressure P can be written:

$$\eta = \frac{\Pi r^4 P t}{8VL} \quad (1)$$

The time that it takes for the liquid to pass between two marks is measured. If h is the distance between the two marked levels and ρ is the density of liquid, then the hydrostatic pressure during the outflow is:

$$P = \rho g h \quad (2)$$

where g is the gravitational acceleration of free fall. We can calibrate the equipment using a reference liquid having a well-known density; in this experiment, we used water as the reference. The dynamic viscosity of the solution is:

$$\eta_s = \frac{\eta_w t_s \rho_s}{t_w \rho_w} \quad (3)$$

where η_s is the viscosity of the test solution (Pas), η_w is the viscosity of water (Pas), t_s is the timing of the runoff of the tested solution (s), t_w is the timing of the runoff of water (s), ρ_s is the density of the test solution (kg m^{-3}) and ρ_w is the density of water (kg m^{-3}).[30] The viscosity was measured by the Oswald viscometer with standard method at 40 °C, even though the electrospinning experiments were carried out under a different temperature. This was to facilitate the time for measurement of the viscosity of high viscous polymer solutions.

Morphological images of the electrospun fibers were carried out using a field emission scanning electron microscope (SEM; Hitachi SU-6600, Tokyo, Japan). High-resolution transmission images were obtained from a transmission electron microscope (TEM, JEOL JEM-2100, Tokyo, Japan) operated at 200 kV to clarify the core–shell structure and to estimate the fiber diameter and wall thickness. The identity of the core and shell materials in the composite fibers were confirmed by an attenuated total reflectance–Fourier-transformed infrared (FTIR) spectroscope (JASCO, ATR–FTIR 4200, JASCO, Tokyo, Japan).

RESULTS AND DISCUSSION

Electrospun fibers prepared by single-nozzle electrospinning

SEM images of the PMMA fibers prepared with different concentrations of PMMA solution are shown in Supplementary Figure S1. At a low concentration of the PMMA solution (3 wt%), only droplets of the polymer solution were observed (as shown in Supplementary Figure S1a). This observation was due to the low viscoelastic force of the PMMA solution, which was not enough to prevent the partial breakup of the charged jet caused by coulombic repulsion when the external voltage was applied.[18] Increasing the concentration of PMMA to 6% (Supplementary Figure S1b) caused a change in morphological appearance from droplets of polymer solution to continuous fibers with an average diameter of 497 nm. However, they still had partially beaded morphology, as shown in the inset of Supplementary Figure S1b. At higher concentrations of PMMA solution, the low solvent content in the solution caused a faster evaporation rate before the solutions reached the collector and higher viscoelastic forces opposed to the columbic forces between positive and negative charges. As a result, an increment of fiber diameters was observed.[31,32] Thus the diameter of the fibers was increased from 932 nm to 1.51 μm when the PMMA polymer solution concentration was increased from 9 to 12 wt% (Supplementary Figures S1c and d).

The morphologies of the electrospun PAN fibers prepared with different concentrations of PAN solution are shown in the SEM images in Supplementary Figure S2. The results showed a similar trend to the PMMA fibers. The fiber diameter increased with increasing polymer concentration. The diameters of the fibers obtained from PAN precursor solution were relatively small compared with the PMMA fibers. Low polymer concentration solutions (that is, 6 and 8 wt%) could produce fibers with very small diameters of 202 and 268 nm, respectively, although many beads could be observed on the fibers. The number of beads was found to decrease from 4.58 to 3.78 beads mm^{-2} when increasing the concentration of PAN solution from 6 to 8 wt%, as shown in Supplementary Figures S2a and b. No beaded

morphology was found when the PAN concentration reached 10 wt%. The average diameters of the electrospun fibers from the PAN solutions with concentrations of 10 and 12 wt% were 422 and 490 nm, respectively. According to these results, the uniform morphology of the single fibers could be obtained using PMMA and PAN solutions with concentrations between 9 and 12 wt% and between 10 and 12 wt% for PMMA and PAN, respectively. Therefore, these concentration ranges were used to study the effect of the absolute viscosities of both polymers and their outer/inner viscosity ratios on the morphology of the core–shell nanofibers in the following experiments.

Viscosity of PMMA and PAN solutions

It is known that solution viscosity is one of the critical elements in determining the morphology of electrospun fibers. The viscosity of the polymer solution is affected by many factors, such as the molecular structure of the polymer, temperature and pressure. Furthermore, the viscosity determines the flow conditions (for example, laminar or turbulent flow) and significantly affects the formation of Taylor cone regimes at the end of the nozzle and the final morphology of the electrospun fibers. Because the viscosity of polymer solutions depends on not only concentration but also temperature and polymer molecular weight, to clarify the net effect of the viscosity ratio on the fiber, all related factors were controlled to keep the same conditions in all experiments. Internal factors, such as the molecular structure or the molecular weight of the polymer, were controlled through the use of the same polymers in the core and shell solutions. The molecular weights of PMMA (core solution) and PAN (shell solution) used in the experiments were 996 000 and 150 000 g mol^{-1}, respectively. Some studies have reported that the viscosity of polymer solutions is an important factor determining the morphology of the obtained fibers. When using different molecular weights of the polymers, adjusting the concentration to give the same polymer solution viscosity allowed them to obtain fibers with the same morphology.[18] The external factors were controlled by using the same experimental conditions, such as gravity force (the electrospinning nozzle was in a horizontal setup, perpendicular to the aluminum foil collector), pressure or applied voltage (15 kV), nozzle-to-collector distance (15 cm), and temperature (all the operations were carried out at an ambient temperature of 25 °C). The absolute viscosity of PAN and PMMA solutions were measured and plotted in Figure 1. From the results, at the same concentration, the viscosity of the PAN solution was higher than that of the PMMA solution. The viscosity of both polymer solutions was increased by increasing the concentration from 93 to 373 mPas for the PMMA solution and from 249 to 677 mPas for the PAN solution. The viscosity ratio for the combinations of PAN and PMMA with different viscosities in this range were then calculated, and their effects on the morphology of the obtained core–shell fibers were investigated.

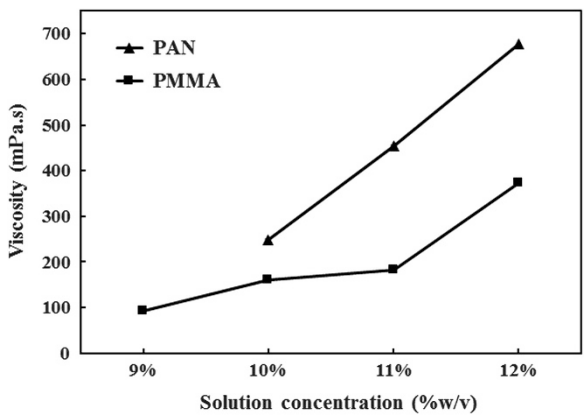

Figure 1 Viscosities of PAN and PMMA solutions at different concentrations.

Electrospun core–shell fibers prepared by coaxial-nozzle electrospinning

In the coaxial-nozzle electrospinning process, the PMMA and PAN solutions were fed into the different channels, and the solutions came into physical contact with each other at the end of the nozzle. To confirm the existence of both the PAN and PMMA portions in the core–shell electrospun fibers, the PAN single fiber and core–shell fiber were characterized by attenuated total reflectance–FTIR spectroscopy. From the FTIR spectra (Figure 2) of the PAN single fibers, vibrational bands of the aliphatic groups (CH_2) on the polymer backbone were observed at approximately 2929 and 1452 cm^{-1}. The signal observed at 2240 cm^{-1} clearly indicated the presence of the nitrile functional group in the chemical structure of PAN. In the FTIR spectra of the composite fibers of PAN and PMMA, the nitrile stretching peak of PAN (2240 cm^{-1}) slightly decreased, while the peaks at 1700, 1485 and 1140 cm^{-1} corresponding to the C=O, O=C–O and C–H groups, respectively, in the chemical structure of PMMA, were clearly seen in the spectra. This result demonstrated that the PMMA core portion was attached quantitatively to the PAN portion in the electrospun core–shell fibers.

In terms of the electrospinnable ranges of viscosity for each single polymer, the viscosity of PMMA solution ranged from 93 to 373 mPas, and the viscosity of the PAN solution ranged from 249 to 677 mPas. These ranges were used to calculate the outer/inner viscosity ratio and study the balance between these ratios and their effects on the morphology of the obtained fibers. The morphology of the core–shell fibers prepared from the PMMA and PAN solutions was observed by SEM, as shown in Figure 3. All composite fibers were observed to be continuously long fibers. However, we could also observe some beaded morphology in almost all combinations of PMMA and PAN with different solution viscosities. When using a constant concentration of PAN, the diameter of the obtained electrospun PAN/PMMA fibers slightly increased with the increase in the viscosity of the PMMA solution. In contrast, when using a constant concentration of PMMA, the average diameters of the electrospun fibers were not significantly different from one another when the viscosity of the PAN solution was increased. After the two polymer solutions came into contact with each other at the end of the nozzle, the core and shell structure transformation was caused by the different phase separation mechanisms.[27] The core diameter and wall thickness of the obtained core–shell fibers could be clearly distinguished, as confirmed by the high-resolution TEM images (Figure 4). From the TEM images, the wall thicknesses of the electrospun core–shell fibers were found to increase when increasing the viscosity ratio of PAN/PMMA. The core–shell nanofiber with the highest viscosity ratio of PAN/PMMA of 4.21 was observed to have very small core diameter, as shown in Figure 4e. At this high viscosity ratio of PAN/PMMA, the core diameter was observed to be a minimum value of 0.53 ± 0.02 μm, and the maximum wall thickness was found to be of 0.79 ± 0.19 μm. These observations were because the viscosity of the shell solution was too high; thus its rigidity obstructed the injection of core solution from the spinneret. When the viscosity ratio of PAN/PMMA was decreased to 2.82, the core diameter of the fibers were observed to be increased, while the wall thickness decreased, as shown in Figures 4d and 5. A uniform core–shell structure was also observed with viscosity ratios

of PAN/PMMA below this value. The decrease in shell viscosity allowed the core PMMA materials to flow out of the spinneret at a higher amount. Moreover, the low viscosity of the shell solution made it easier to elongate the electrostatic repulsion between the surface charges during electrospinning process. However, the shell solution viscosity should be high enough to maintain the coaxial structure of the solution jet from the injection nozzle until full solidification.[33] At a too-low viscosity ratio of PAN/PMMA of 0.67, we could observe unstable core–shell structures, as shown in Figure 4a. These phenomena were ascribed to the fact that the viscosities of the core and shell were nearly the same (namely, the viscosity ratio is nearly 1.0). The viscosity of PMMA solution (373 mPas) was high enough to overcome the viscosity of the PAN solution (249 mPas), which meant that the shell solution could not stabilize the compound Taylor cone (the conical shape that occurred at the end of the nozzle). This unstable state of the electrospinning fluid jet followed along the pathway until it reached the aluminum foil collector as a rigid fiber. The twisting of the core morphology was observed as shown in the illustration model in Figure 4f. At a low viscosity ratio of PAN/PMMA, the twisting of the core morphology was due to the high surface tension between the two layers of polymer, which overcame the viscoelastic force in the shell solution. In other words, the shell solution viscosity was too low to stabilize the core–shell morphology. When increasing the viscosity ratio of PAN/PMMA, the shell solution not only was more stable but also obstructed the flow of the core solutions out of the spinneret, resulting in the smaller core diameter of the fibers.

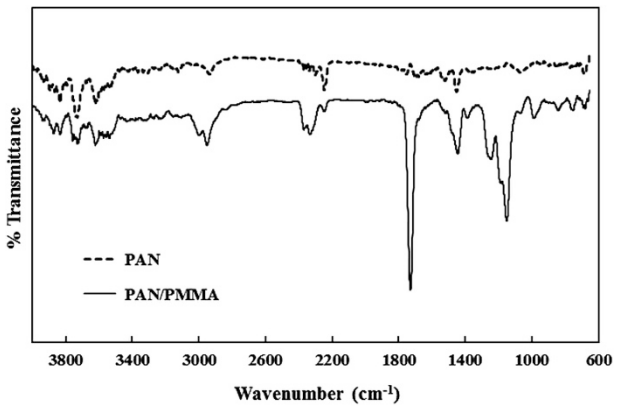

Figure 2 FTIR spectra of PAN and PAN/PMMA fibers.

Figure 5 shows the dependence of the total diameter, core diameter and wall thickness of the PAN/PMMA nanofibers on the viscosity ratio of PAN/PMMA. The total diameter was found to increase with the increasing viscosity ratio of PAN/PMMA, while the core diameter and wall thickness seemed to be rather scattered. This result may be caused by the nonuniform core–shell structure of the fibers at the viscosity

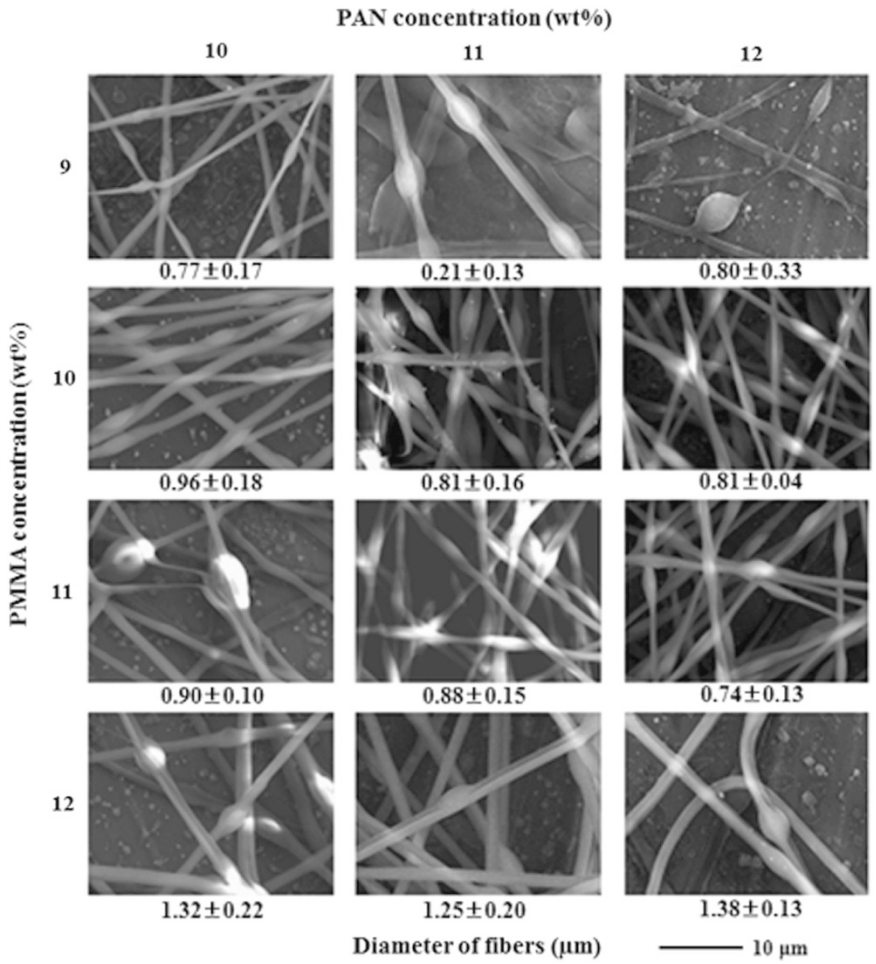

Figure 3 SEM images of electrospun PAN/PMMA nanofibers prepared with different PAN and PMMA concentrations.

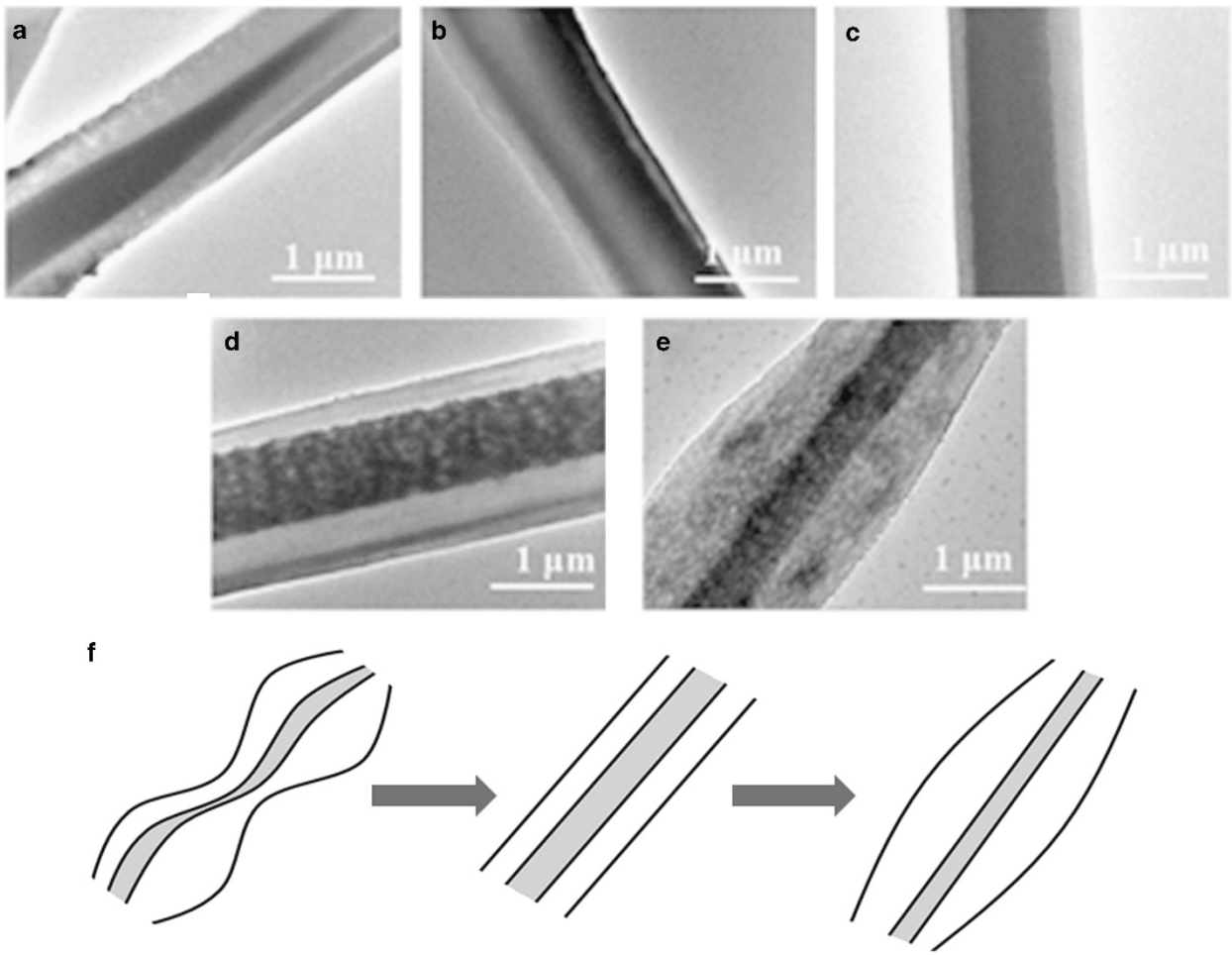

Figure 4 TEM images of the electrospun PAN/PMMA nanofibers prepared with various viscosity ratios of PAN/PMMA: (**a**) 0.67; (**b**) 1.22; (**c**) 1.81; (**d**) 2.82; (**e**) 4.21; and (**f**) schematic illustration of core–shell morphology when increasing the PAN/PMMA viscosity ratio.

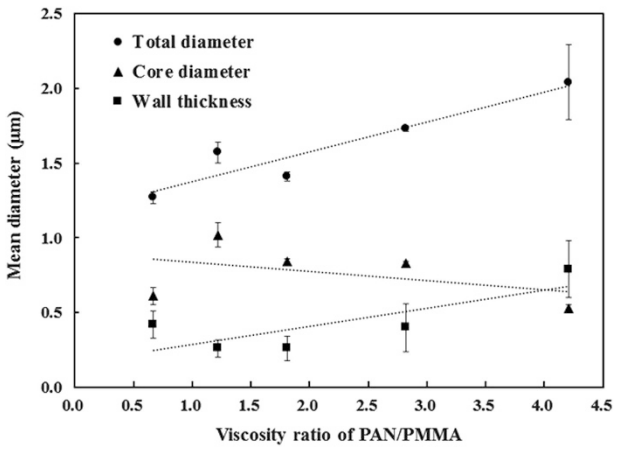

Figure 5 Dependence of total diameter, core diameter and wall thickness of PAN/PMMA nanofibers on the PAN/PMMA viscosity ratio.

ratio of PAN/PMMA of 0.67. If we omit the results of core diameter and wall thickness of the fibers, which were unstable, fabricated from this lowest viscosity ratio (0.67), then the core diameter of the fibers seemed to gradually decrease and the wall thickness increased linearly when increasing the viscosity ratio of PAN/PMMA. From the TEM images, the viscosity ratio of PAN/PMMA at 1.22 was found to be the optimal minimum value to fabricate the uniform core–shell structure along the long axis of the fibers. At this viscosity ratio, a minimum wall thickness of the core–shell fibers ($0.26 \pm 0.06\,\mu m$) and a maximum core diameter ($1.02 \pm 0.08\,\mu m$) could be observed. Based on this research, the range of outer/inner viscosity ratio should be 1.22–2.82 within the electrospinnable range of both the core and shell polymer solutions. One benefit of determining the optimal range of the outer/inner viscosity ratio from this work is that the different viscosities of the outer and inner polymer solutions also had an effect. For example, with the same outer/inner viscosity ratio, the lower absolute viscosity of the outer and inner polymer solution would lead to the fabrication of smaller total diameter fibers compared with the fibers fabricated from higher absolute viscosity outer and inner polymer solutions. However, the same core–shell fibers with good morphology could be fabricated in both cases. These ranges of PAN/PMMA viscosity ratios could be suitable for application to other polymer systems or to other applications that require a higher specific surface area (resulting from a thinner wall thickness), such as the preparation of hollow fibers as substrates for photocatalysts or hollow carbon fibers as electrodes for supercapacitors or photovoltaic cells.

CONCLUSION

The effect of the viscosity ratio of PAN/PMMA solution on the morphology of the core–shell fibers, including the total diameter, core

diameter and wall thickness, were investigated. The viscosity ratio of PAN/PMMA used to prepare the uniform core–shell structure was optimized to be in the range of 1.22–2.82. At the minimum viscosity ratio of PAN/PMMA of 1.22, the electrospun core–shell fibers show the thinnest wall diameter of 0.26 ± 0.06 μm, which could be suitable for any applications that require electrospun fibers with high specific surface area.[34] Moreover, the core diameter and wall thickness of the core–shell fibers could be controlled by changing the viscosity ratio between the shell and the core solutions. The range of suitable viscosities of the shell/core solutions obtained from this work could be applicable to the preparation of electrospun fibers from other combinations of polymer solutions for various applications by measuring the dynamic viscosity of the selected polymer solutions using the same method and adjusting their outer/inner viscosity ratio.

ACKNOWLEDGEMENTS

We thank Dr T Yabutsuka of the Graduate School of Energy Science, Kyoto University for the utilization of the SEM apparatus. We also thank Professor Y Tsujii and Dr K Sakakibara of Institute for Chemical Research, Kyoto University for giving us the opportunity to use the TEM system.

1 Zhang, Y., Huang, Z.-M., Xu, X., Lim, C. T. & Ramakrishna, S. Preparation of core-shell structured PCL-r-Gelatin bi-component nanofibers by coaxial electrospinning. *Chem. Mater.* **16**, 3406–3409 (2004).
2 Feng, Y., Zhang, Y. Z., Yong, T. & Ramakrishna, S. A novel biodegradable system based on BSA/PCL core-shell structured nanofibers for controlled drug delivery. *NSTI Nanotech* **2**, 377–380 (2006).
3 Xu, Q., Yu, X., Liang, Q., Bai, Y., Huang, Z.-H. & Kang, F. Nitrogen-doped hollow activated carbon nanofibers as high performance supercapacitor electrodes. *J. Electroanal. Chem.* **739**, 84–88 (2015).
4 Wu, Y., Gao, M., Li, X., Liu, Y. & Pan, H. Preparation of mesohollow and microporous carbon nanofiber and its application in cathode material for lithium–sulfur batteries. *J. Alloys Comp.* **608**, 220–228 (2014).
5 Liu, B., Yu, Y., Chang, J., Yang, X., Wu, D. & Yang, X. An enhanced stable-structure core-shell coaxial carbon nanofiber web as a direct anode material for lithium-based batteries. *Electrochem. Commun.* **13**, 558–561 (2011).
6 Chen, Y., Lu, Z., Zhou, L., Mai, Y. W. & Huang, H. Triple-coaxial electrospun amorphous carbon nanotubes with hollow graphitic carbon nanospheres for high-performance Li ion batteries. *Energy Environ. Sci.* **5**, 7898–7902 (2012).
7 Park, S.-H., Jung, H.-R. & Lee, W.-J. Hollow activated carbon nanofibers prepared by electrospinning as counter electrodes for dye-sensitized solar cells. *Electrochim. Acta.* **102**, 423–428 (2013).
8 El-Deen, A. G., Barakat, N. A. M., Khalild, K. A. & Kim, H. Y. Hollow carbon nanofibers as an effective electrode for brackish water desalination using the capacitive deionization process. *New J. Chem.* **38**, 198–205 (2014).
9 Wang, J., Liu, Q., Gao, Y., Wang, Y., Guo, L. & Jiang, G. High-throughput and rapid screening of low-mass hazardous compounds in complex samples. *Anal. Chem.* **87**, 6931–6936 (2015).
10 Kim, S., Kim, M., Kim, Y. K., Hwang, S.-H. & Lim, S. K. Core–shell-structured carbon nanofiber-titanate nanotubes with enhanced photocatalytic activity. *Appl. Catal. B Environ.* **148–149**, 170–176 (2014).
11 Miyauchi, M., Miao, J., Simmons, T. J., Lee, J.-W., Doherty, T. V., Dordick, J. S. & Linhardt, R. J. Conductive cable fibers with insulating surface prepared by coaxial electrospinning of multiwalled nanotubes and cellulose. *Biomacromolecules* **11**, 2440–2445 (2010).
12 Miao, J., Miyauchi, M., Dordick, J. S. & Linhardt, R. J. Preparation and characterization of electrospun core sheath nanofibers from multi-walled carbon nanotubes and poly (vinyl pyrrolidone). *J. Nanosci. Nanotechnol.* **12**, 2387–2393 (2012).
13 Qu, H., Wei, S. & Guo, Z. Coaxial electrospun nanostructures and their applications. *J. Mater. Chem. A* **1**, 11513–11528 (2013).
14 Zander, N. E., Strawhecker, K. E., Orlicki, J. A., Rawlett, A. & Beebe, M. T. P. Jr. Coaxial electrospun poly(methyl methacrylate)-polyacrylonitrile nanofibers: atomic force microscopy and compositional characterization. *J. Phys. Chem. B* **115**, 12441–12447 (2011).
15 Kim, C., Jeong, Y. I., Ngoc, B. T. N., Yang, K. S., Kojima, M., Kim, Y. A., Endo, M. & Lee, J. W. Synthesis and characterization of porous carbon nanofibers with hollow cores through the thermal treatment of electrospun copolymeric nanofiber webs. *Small* **3**, 91–95 (2007).
16 Hong, C. K., Yang, K. S., Oh, S. H., Ahn, J.-H., Cho, B.-H. & Nah, C. Effect of blend composition on the morphology development of electrospun fibres based on PAN/PMMA blends. *Polym. Int.* **57**, 1357–1362 (2008).
17 Lee, B.-S., Jeon, S.-Y., Park, H., Lee, G., Yang, H.-S. & Yu, W.-R. New electrospinning nozzle to reduce jet instability and its application to manufacture of multi-layered nanofibers. *Sci. Rep.* **4**, 6758–6766 (2014).
18 Chuangchote, S., Sagawa, T. & Yoshikawa, S. Electrospinning of poly(vinyl pyrrolidone): effects of solvents on electrospinnability for the fabrication of poly(p-phenylene vinylene) and TiO_2 nanofiber. *J. Appl. Polym. Sci.* **114**, 2777–2791 (2009).
19 Supaphol, P. & Chuangchote, S. On the electrospinning of poly(vinyl alcohol) nanofiber mats: a revisit. *J. Appl. Polym. Sci.* **108**, 969–978 (2008).
20 Gomes, D. S., Silva, da, A. N. R., Morimoto, N. I., Mendes, L. T. F., Furlan, R. & Ramos, I. Characterization of an electrospinning process using different PAN/DMF concentrations. *Polímeros* **17**, 206–211 (2007).
21 Jalili, R., Morshed, M. & Ravandi, S. A. H. Fundamental parameters affecting electrospinning of PAN nanofibers as uniaxially aligned fibers. *J. Appl. Polym. Sci.* **101**, 4350–4357 (2006).
22 Martinez, R. D., Silva, da, A. N. R., Furlan, R., Ramos, I. & Santiago-Avilés, J. J. Analysis of electrospinning of nanofibers as a function of polyacrylonitrile (PAN) concentration. *J. Integr. Circuits Syst.* **1**, 48–51 (2006).
23 Bedi, J. S., Lester, D. W., Fang, Y. X., Turner, J. F. C., Zhou, J., Alfadul, S. M., Perry, C. & Chen, Q. Electrospinning of poly(methyl methacrylate) nanofibers in a pump-free process. *J. Polym. Eng.* **33**, 453–461 (2013).
24 Raza, A., Wang, J., Yang, S., Si, Y. & Ding, B. Hierarchical porous carbon nanofibers via electrospinning. *Carbon Lett.* **15**, 1–14 (2014).
25 Li, L., Jiang, Z., Li, M., Li, R. & Fang, T. Hierarchically structured PMMA fibers fabricated by electrospinning. *RSC Adv.* **4**, 52973–52985 (2014).
26 Yu, J. H., Fridrikh, S. V. & Rutledge, G. C. Production of submicrometer diameter fibers by two-fluid electrospinning. *Adv. Mater.* **16**, 1562–1566 (2004).
27 Lee, G. H., Song, J.-C. & Yoon, K.-B. Controlled wall thickness and porosity of polymeric hollow nanofibers by coaxial electrospinning. *Macromol. Res.* **18**, 571–576 (2010).
28 Pham, U. H. T., Hanif, M., Asthana, A. & Iqbal, S. M. A microfluidic device approach to generate hollow alginate microfibers with controlled wall thickness and inner diameter. *J. Appl. Phys.* **117**, 214703 (2015).
29 Sun, Z., Zussman, E., Yarin, A. L., Wandorff, J. H. & Greiner, A. Compound core–shell polymer nanofibers by co-electrospinning. *Adv. Mater.* **15**, 1929–1932 (2003).
30 Joseph, K., Mordechai, S. & William, A. W. Viscosity of liquid water in the range −8 °C to 150 °C. *J. Phys. Chem. Ref. Data* **7**, 941–948 (1978).
31 Srivastava, Y., Marquez, M. & Thorsen, T. Multijet electrospinning of conducting nanofibers from microfluidic manifolds. *J. Appl. Polym. Sci.* **106**, 3171–3178 (2007).
32 Wang, N., Burugapalli, K., Song, W., Halls, J., Moussy, F., Zheng, Y., Ma, Y., Wu, Z. & Li, K. Tailored fibro-porous structure of electrospun polyurethane membranes, their size-dependent properties and trans-membrane glucose diffusion. *J. Membr. Sci.* **427**, 207–217 (2013).
33 Li, D. & Xia, Y. Direct fabrication of composite and ceramic hollow nanofibers by electrospinning. *Nano Lett.* **4**, 933–938 (2004).
34 Kaerkitcha, N., Chuangchote, S. & Sagawa, T. Control of physical properties of carbon nanofibers obtained from coaxial electrospinning of PMMA and PAN with adjustable inner/outer nozzle-ends. *Nanoscale Res. Lett.* **11**, 1–9 (2016).

Supplementary Information accompanies the paper on Polymer Journal website (http://www.nature.com/pj)